Current Research in Toxicology 2 (2021) 386–398

Contents lists available at ScienceDirect

Current Research in Toxicology

journal homepage: www.elsevier.com/locate/crtox

The new psychoactive substances 25H-NBOMe and 25H-NBOH induce abnormal development in the zebrafish embryo and interact in the DNA major groove

Wellington Alves de Barros [a], Camila da Silva Nunes [b], Juliana Alves da Costa Ribeiro Souza [c], Igor José dos Santos Nascimento [b], Isis Martins Figueiredo [b], Thiago Mendonça de Aquino [b], Leonardo Vieira [c], Davi Farias [c], Josué Carinhanha Caldas Santos [b,*], Ângelo de Fátima [a,*]

[a] Departamento de Química, Instituto de Ciências Exatas, Universidade Federal de Minas Gerais, Belo Horizonte, MG, Brazil
[b] Instituto de Química e Biotecnologia, Universidade Federal de Alagoas, Maceió, AL, Brazil
[c] Departamento de Biologia Molecular, Universidade Federal da Paraíba, João Pessoa, PB, Brazil

ARTICLE INFO

Handling Editor: Thomas Knudsen

Keywords:
Phenethylamines
Recreational drugs
DNA interaction
Malformation
Embryo mortality

ABSTRACT

Toxicological effects of 25H-NBOMe and 25H-NBOH recreational drugs on zebrafish embryos and larvae at the end of 96 h exposure period were demonstrated. 25H-NBOH and 25H-NBOMe caused high embryo mortality at 80 and 100 μg mL^{-1}, respectively. According to the decrease in the concentration tested, lethality decreased while non-lethal effects were predominant up to 10 and 50 μg mL^{-1} of 25H-NBOH and 25H-NBOMe, respectively, including spine malformation, egg hatching delay, body malformation, otolith malformation, pericardial edema, and blood clotting. We can disclose that these drugs have an affinity for DNA *in vitro* using biophysical spectroscopic assays and molecular modeling methods. The experiments demonstrated that 25H-NBOH and 25H-NBOMe bind to the unclassical major groove of ctDNA with a binding constant of 27.00 × 10^4 M^{-1} and 5.27 × 10^4 M^{-1}, respectively. Furthermore, these interactions lead to conformational changes in the DNA structure. Therefore, the results observed in the zebrafish embryos and DNA may be correlated.

Introduction

The zebrafish (*Danio rerio*) model organism is progressively used for measuring drug toxicity and/or safety, and abundant studies have endorsed that mammalian, and zebrafish toxicity profiles are strikingly comparable (Cassar et al., 2020; Dai et al., 2014; Keshari et al., 2016; Ko et al., 2009; McGrath and Li, 2008; Stewart et al., 2011). In addition, zebrafish have high genetic homology to humans, genetic tractability, low cost, and hence usefulness in high-throughput analyses (Cassar et al., 2020; Stewart et al., 2013). These non-traditional model organisms have effectively demonstrated complex processes involved in drug abuse responses (Mathur and Guo, 2010; Stewart et al., 2011). Neurobehavioral studies specifically established or accepted for zebrafish provide useful methods to explore reinforcing properties of drugs and to study drug use related phenomena, including sensitization, tolerance, withdrawal, drug-seeking, extinction, and relapse (Braida et al., 2007; Cachat et al., 2010; Kily et al., 2008; Petzold et al., 2009). However, the use of zebrafish as a model to evaluate the potential toxicity of recreational drugs is still little explored. For instance, exposure to ketamine (50–90 μg mL^{-1}) for 24 h resulted in morphological and behavioral changes in zebrafish, with higher embryo mortality, skeletal deformities, and a reduction in body length. Malformation levels were higher in the groups exposed to the drug than the control, observing a higher incidence of the distended thoracic region and trunk abnormalities such as lordosis or kyphosis (Félix et al., 2017). In another study, cocaine (10–20 mg L^{-1}) exposure resulted in a decreased telencephalic area in a dose-dependent fashion in embryonic brains of zebrafish and an elevated heart rate 37% above untreated fish (Mersereau et al., 2016). In this sense, the zebrafish model may not only serve as a valuable tool for screening for drug use and their abuse-related responses but also for the toxicity of drug abuse effects, especially in the case of new psychoactive substances (NPS) NBOMes/NBOHs in which practically non-existent data are reported regarding these later possible effects.

Recreational drugs are legal and illegal substances used without a medical reason to induce an altered state of consciousness for pleasure

* Corresponding authors.
E-mail addresses: josue@iqb.ufal.br (J.C.C. Santos), adefatima@qui.ufmg.br (Ă. de Fátima).

https://doi.org/10.1016/j.crtox.2021.11.002
Received 29 July 2021; Revised 19 October 2021; Accepted 18 November 2021

(Miller et al., 2015; Ropero-Miller and Goldberger, 1998). However, these drugs are dangerous in any situation and may have devastating effects that include acute toxicity reactions and death (Andreasen et al., 2015; Morini et al., 2017; Ropero-Miller and Goldberger, 1998; Vale, 2012). The growing recreational consumption of NPS not only undeniably signifies an unprecedented challenge in the field of drug addiction but also a fast-rising problem from social, cultural, legal, health, and political perspectives (Bersani et al., 2014; Corazza et al., 2013; Larson and Bammer, 1996). For instance, prior to 2010, essentially no history of the human use of NPS known as NBOMes/NBOHs (Fig. 1) had been recorded (Andreasen et al., 2015); however, after their introduction, these substances have been associated with intoxication and fatal incidents (Andreasen et al., 2015; Kristofic et al., 2016; Kueppers and Cooke, 2015; Lawn et al., 2014; Lowe et al., 2015; Morini et al., 2017; Poklis et al., 2014; Wood et al., 2015).

25H-NBOH and 25H-NBOMe are substituted phenethylamines bearing methoxy groups on the 2 and 5 positions of the A ring and a hydroxyl (NBOH) or methoxy group (NBOMe) in position 1′ in the B ring (Fig. 1). The hallucinogenic effects of these substances are due to their agonistic effects on serotonin 5-HT_{2A} receptors (5-HT_{2A}R). Indeed, some of these reactional drugs possess the highest agonistic effects to 5-HT_{2A}R, which means that very low doses are needed to achieve the powerful hallucinogenic effects compared with lysergic acid diethylamide (LSD) or ecstasy (Cassar et al., 2020; Lowe et al., 2015). NBOMes/NBOHs are often marketed as “legal” LSD and sometimes misidentified as ecstasy (Corazza et al., 2013; Ninnemann and Stuart, 2013). Thus, this poses a significant safety concern when users think they are taking LSD and/or ecstasy but are essentially ingesting NBOMes/NBOHs because the symptoms can prove to be more severe and need an advanced level of attention from medical professionals (Lowe et al., 2015). In fact, unlike NBOMes/NBOHs, LSD and ecstasy are rarely directly attributable to death. Moreover, knowledge about the toxicology of LSD or ecstasy, or even cocaine, is well established (Alvarenga et al., 2010; Barenys et al., 2009; Dishotsky et al., 1971; Jih-Heng and Lih-Fang, 1998; Nichols and Grob, 2018; Polifka and Friedman, 1991), while very limited or practically non-existent data are reported for NBOMes/NBOHs (Arantes et al., 2017; de Barros et al., 2021a; Machado et al., 2020). 25I-NBOMe was detected, after death, in blood (from 0.04 to 0.95 nM), urine (6.69 nM), vitreous humor (0.23 nM); 25C-NBOMe was detected in blood (1.49 nM) and urine (6.85 nM), and 25B-NBOMe detected in blood samples (4.18 nM) (Andreasen et al., 2015; Kueppers and Cooke, 2015; Lowe et al., 2015; Morini et al., 2017; Poklis et al., 2014; Shanks et al., 2015; Tang et al., 2014). However, little has been studied about the toxicity of these substances, and their possible effects on pregnancy.

Based on the potential of zebrafish to assess the toxicity of recreational drugs and the lack of reports on such effects induced by NBOMes and NBOHs, herein we describe the 25H-NBOH and 25H-NBOMe toxicity on the zebrafish model. It is important to point out that the results with zebrafish often turned out to differ with respect to concentration and efficacy, in this way the doses used in this study and elsewhere may be different and have different effects. Finally, we have also performed molecular modeling studies and biophysical interaction *in vitro* of the above-mentioned recreational drugs with the *Calf thymus* DNA (model), which is characterized as a biological target related to toxicity effects.

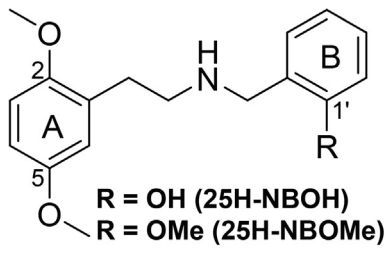

Fig. 1. Representative chemical structure of 25H-NBOH and 2H-NBOMe recreational drugs.

Material and methods

In vivo assays with zebrafish embryos

Zebrafish embryos

The zebrafish (*Danio rerio*) embryos were provided by the zebrafish facility established at the Department of Molecular Biology, Federal University of Paraiba (João Pessoa, Brazil). Zebrafish adults (wild-type strain) were kept at 26 ± 1 °C under a 14:10 h (light:dark) photoperiod. The water quality was maintained by activated-carbon filtration, conductivity at 750 ± 50 μS, and dissolved oxygen above 95% saturation. Fishes were fed daily with commercial food (Tropical Gran Discus, Sarandi, Brazil) and *Artemia* sp. nauplii and monitored for abnormal behavior or disease development.

An egg trap was placed overnight in a tank containing male and female specimens (1:1 ratio) one day before testing to obtain embryos. One hour after beginning the light cycle, eggs were collected with a Pasteur pipette and rinsed with E3 medium (5 mM NaCl, 0.17 mM KCl, 0.33 mM $CaCl_2$, and 0.33 mM $MgSO_4$) for subsequent selection of embryos by using a stereomicroscope (80 × magnification). Viable fertilized eggs were selected for embryotoxicity assays. The Ethics Commission approved all experiments conducted with zebrafish in this study in Animal Use in Research (CEUA 4460140920) of the Federal University of Paraiba.

Acute toxicity test using zebrafish embryos

The Fish Embryo Acute Toxicity (FET) test was independently conducted with 25H-NBOH and 25H-NBOMe according to the OECD's guideline number 236 (OECD, 2013) with modifications. Zebrafish embryos up to 3 h post-fertilization (hpf) of age were exposed to five crescent concentrations of 25H-NBOH (5, 10, 20, 40, and 80 μg mL^{-1}) and 25H-NBOMe (5, 20, 50, 70, and 100 μg mL^{-1}). Each concentration tested was prepared in a 96-well plate containing 20 fertilized eggs (1 embryo per well) exposed to the test sample, and 4 embryos were exposed only to E3 medium (internal controls). An additional plate containing embryos exposed to E3 medium was also assayed. The exposure was performed for 96 h, and the embryos were analyzed every 24 h for the apical endpoints: egg coagulation; lack of somite formation, lack of detachment of the tail-bud from the yolk sac; and lack of heartbeat. The embryo/larva was considered dead in the presence of any of these endpoints. The number of deaths was used to calculate the LC_{50} (median lethal concentration). Additionally, sublethal effects were also recorded daily: eye malformation, otolith malformation; mouth malformation; spine malformation; body pigmentation; egg hatching delay, yolk sac edema, body malformation, pericardial edema; head edema; blood clotting; and undersize. The exposures were under static conditions (without renovation of the test sample or E3 medium). Observations were performed in a stereomicroscope (80 × magnification) and photographed (Zeiss). Surviving larvae were euthanized after 96 h with eugenol and properly discarded.

Statistical analysis

The median lethal concentration (LC_{50}) values were calculated by *probit* regression analysis (Finney, 1971). A one-way ANOVA completed with Tukey's posthoc comparison determined differences to independently compare each exposure group to the control group. The $p < 0.05$ was considered statistically significant.

In vitro interaction assays of ctDNA and 25H-NBOH/25H-NBOMe

Reagents and solutions

All reagents used were chemically pure. The solutions were prepared with ultrapure water with a specific resistivity of 18.2 MΩ × cm from a Milli-Q® purification system (Millipore, Bedford, MA, USA). The ctDNA solution was prepared by dissolving an appropriate amount of sodium salt of DNA *Calf thymus* type I (Sigma Aldrich, USA) in Tris-HCl buffer (10 mM, pH = 7.40, 100 mM of NaCl); the solution was left under magnetic stirring for 24 h, followed by 30 min in an ultrasonic bath (Quimis model Q335D, Brazil). The ctDNA concentration was determined by absorbance at 260 nm using molar extinction coefficient ε_{260} = 6600 $M^{-1}cm^{-1}$. The ctDNA solution's purity was determined by the absorbance ratio at 260 and 280 nm (A_{260}/A_{280}), where a value between 1.8 and 1.9 indicates that the ctDNA solution was sufficiently free of proteins (Savariz et al., 2014). The stock solution of ligands 25H-NBOH and 25H-NBOMe was prepared by dissolving 10 mg of each substance in 4 mL of DMSO; the subsequent dilution was prepared in the Tris-HCl buffer. The potassium iodide solution was prepared in ultrapure water to a final concentration of 0.3 M of KI and 5 mM $Na_2S_2O_3$. The green methyl (MG) probe solution was prepared by dissolving 10 mg of MG in 5 mL of ultrapure water and then extracted with chloroform (5 × 5 mL) to remove traces of the violet methyl impurity (Prieto et al., 2014). The concentration of the impurity-free solution was determined by the absorbance at 631 nm using the molar extinction coefficient of 85300 $M^{-1}cm^{-1}$ (Kim and Nordén, 1993). For the ^{1}H NMR experiment, 5 mM phosphate buffer pH 7.40 prepared in D_2O (99.9%) was used. The ligands' stock solutions were prepared in DMSO d_6 and diluted in the buffer so that the maximum concentration of DMSO d_6 was not more than 20% (v/v). Sodium trimethylsilyl propionate at 2.5 mM (TMSP, Cambridge Isotope Laboratories) was used as an internal standard for chemical displacement for a final volume of 600 μL.

UV–vis absorption measurements

The molecular absorption measurements were performed in a scanning spectrophotometer Micronal (AJX-6100PC, Brazil) with double-beam equipped quartz cuvettes of 10 mm optical path. The absorbance signal of ligands (20 μM) was evaluated in the absence and presence of ctDNA (20 μM), as well as the absorbance of the ctDNA free (20 μM). The spectrophotometric measurement was performed in the 200-340 nm range. In the melting temperature assay, the absorbance of the ctDNA solution (20 μM) in the absence and presence of ligands (20 and 100 μM) was monitored at 260 nm, slowly heated from 25 to 100 °C using a heating system model SP12/200ED (SPlabor, Brazil).

Molecular fluorescence studies

Molecular fluorescence measurements were performed on a Shimadzu spectrofluorometer (model 5301PC, Japan) equipped with a Xenon lamp (150 W) using quartz cuvettes of a 10 mm optical path. Spectrofluorometric titrations were performed by maintaining the concentration of ligands at 7.5 μM, increasing amounts of ctDNA (0–250 μM). The titration was carried out at three different temperatures (23, 30, and 37 °C) to determine the binding and thermodynamics parameters. The influence of ionic strength was determined by spectrofluorimetric titration at different NaCl concentrations (0, 25, 50, 100, and 200 mM). Mathematical corrections were made when necessary to correct the inner filter effect. Titrations using potassium iodide (KI) and the DNA probes DAPI, Hoechst (HO), ethidium bromide (EB), acridine orange (AO), thiazole orange (TO), berberine (BB), and methyl green (MG) were used to determine the preferential binding mode. The ligands in the KI assay were titrated with increasing concentrations of KI (0, 5, 10, 25, 50, 75, and 120 μM) in the absence and presence of two excesses of ctDNA (50 and 100 μM). The emission spectra in experiments with DAPI, HO, EB, AO, TO, and BB were obtained by fixing the probe concentration (2 μM) and ctDNA (10 μM); finally, the titration with 25H-NBOH or 25H-NBOMe (0–120 μM) was performed. The spectra were obtained from excitation at specific wavelength for each probe: DAPI (λ_{ex} = 358 nm, λ_{em} = 455 nm), Hoescht (λ_{ex} = 353 nm, λ_{em} = 452 nm), ethidium bromide (λ_{ex} = 525 nm, λ_{em} = 592 nm), acridine orange (λ_{ex} = 490 nm, λ_{em} = 524 nm), thiazole orange (λ_{ex} = 500 nm, λ_{em} = 526 nm), and berberine (λ_{ex} = 356 nm, λ_{em} = 525 nm). In the MG experiment, the ligands (7.5 μM) were titrated with increasing concentrations of ctDNA in the absence and presence of methyl green (0, 10, and 20 μM). All spectra were recorded from 280 to 450 nm by exciting at 260 nm (slit 5 and 10 nm for excitation and emission).

Circular dichroism studies

The circular dichroism spectra measurements were performed on a Jasco spectropolarimeter (model J-815, Japan) equipped with a Peltier-type temperature adjustment system in a quartz cuvette 0.1 mm optical path. The measurements were made in the UV region in the range of 190–240 nm at 25 °C in the presence of N_2 (99.99%). The ctDNA (100 μM) was titrated in increments of ligands (100, 200, and 300 μM). Each spectrum corresponds to the average of four scans at 50 nm min^{-1}.

NMR studies

The ^{1}H NMR spectra were obtained on a Bruker Avance 600 MHz spectrometer equipped with a 5 mm indirect detection probe (Santana et al., 2019). The spectra were calibrated with internal standard TPMS. The ligand concentration was fixed (1 mM), and the spectra were recorded in the absence and presence of ctDNA (0.01 and 0.04 mM) using 32 scans.

Molecular modeling

For the molecular modeling studies, the co-crystallized structure of the dodecameric DNA was taken from the Protein Data Bank (PDB id: 1G3X) (Malinina et al., 2002). The studied drugs 25H-NBOH and 25H-NBOMe were built using MarvinSketch® software program (Csizmadia, 1999), and the protonation states for each compound at pH 7.4 were considered. The compounds' geometries were optimized in the gas-phase using the semi-empirical method AM1 (Austin Model), and the angle and length of the connection were corrected by using ORCA® software (Neese, 2012). Molecular docking was performed using GOLD® software (Verdonk et al., 2003) to study the interactions of 25H-NBOH and 25H-NBOMe. Hydrogens atoms were added and water molecules were removed for the DNA structure. All of the DNA structure was selected (70 Å), and the ligands were docked using the Astex Statistical Potential (ASP) algorithm (Lozano Untiveros et al., 2019; Passos et al., 2020; Santana et al., 2019). Finally, the optimal binding poses were selected for analysis and were chosen as the initial conformation for molecular dynamics (MD) simulations performed at 100 ns using the GROMACS® software program (Braga et al., 2019; Roque Marques et al., 2019). The interaction poses were visualized by using the UCSF Chimera software program. The RMSD values during the simulation were calculated employing GROMACS®, and RMSD plots were generated using the Xmgrace® software program (Braga et al., 2019).

Results and discussion

In vivo assays with zebrafish embryos

25H-NBOH and 25H-NBOMe used in this work were previously prepared by our research group, according to de Barros et al. (2021b). Fig. 2 shows an overview of the effects of compounds tested on zebrafish embryos and larvae at the end of a 96 h exposure period. Both samples caused high embryo mortality at the highest concentrations tested (80 and 100 μg mL^{-1} of 25H-NBOH and 25H-NBOMe,

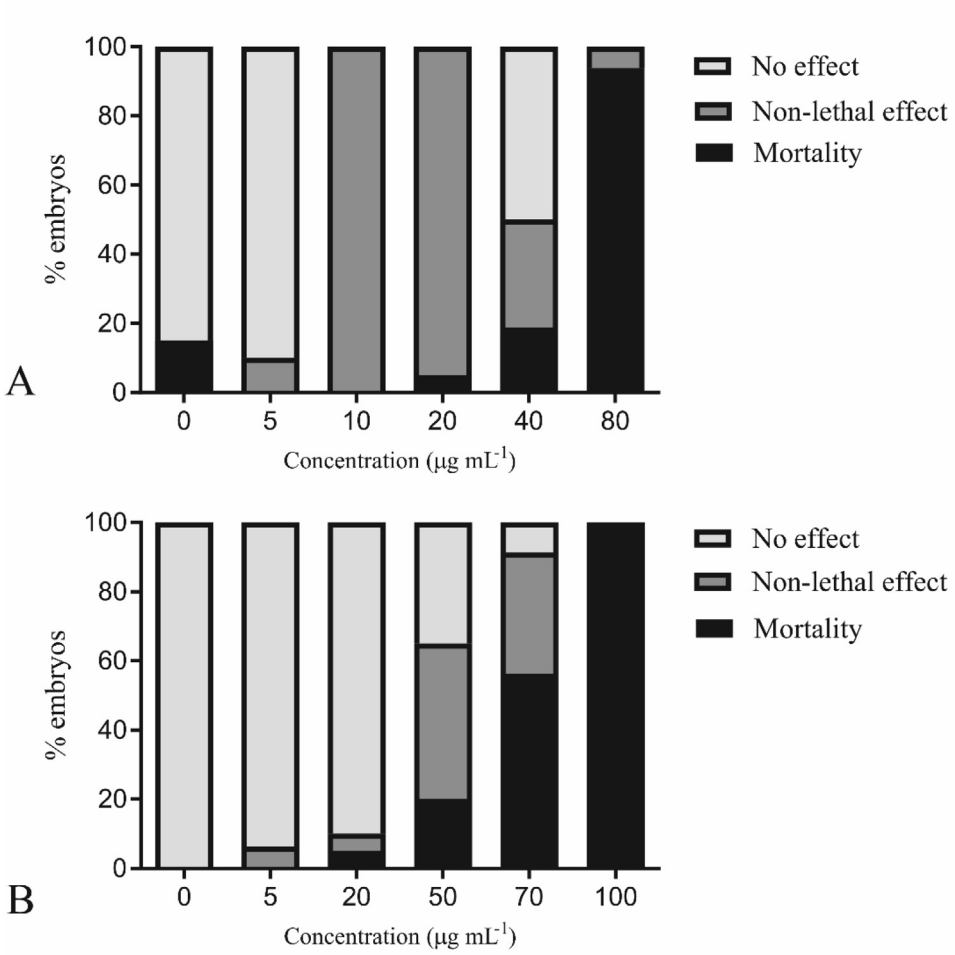

Fig. 2. A general overview of (A) 25H-NBOH and (B) 25H-NBOMe cumulative effects on zebrafish embryos and larvae (n = 20 / concentration) after 96 h of exposure. No effect: morphological characteristics similar to the control organisms; Non-lethal effect: the presence of sublethal endpoints; Mortality: the presence of lethality endpoints.

respectively) (Fig. 2A-B). The embryos and larvae showed no morphological changes at lower concentrations (Fig. 3A-C). Coagulation was the only endpoint of lethality observed for both samples (Fig. 3D-E). According to the decrease in the concentration tested, lethality decreased while non-lethal effects were predominant up to 10 and 50 μg mL^{-1} of 25H-NBOH and 25H-NBOMe, respectively. The non-lethal effects observed were spine malformation, egg hatching delay, and body malformation for both samples, while otolith malformation, pericardial edema, and blood clotting were only found for 25H-NBOMe (Fig. 3).

Table 1 shows the embryotoxicity assay results in zebrafish embryos exposed to increasing concentrations of 25H-NBOH and 25H-NBOMe. The compounds showed specific toxicity profiles to zebrafish embryos. 25H-NBOH was more lethal (LC_{50} 43 μg mL^{-1}) than 25H-NBOMe (LC_{50} 84 μg mL^{-1}). However, both samples' lethality endpoints could only be verified in high concentrations, as previously discussed. Therefore, this contrasts with the sublethal endpoints that appeared in lower concentrations, and again 25H-NBOH was the most toxic sample (Table 1). The lower LOAEL (Lowest-observed-adverse-effect level) value for 25H-NBOH was 10 μg mL^{-1} for the spine malformation endpoint (Fig. 3h), while for 25H-NBOMe it was 50 μg mL^{-1} for spine malformation and blood clotting (Fig. 3i-j). Although the samples only display lethal effects in higher concentrations, their sublethal effects, most accounting for teratogenicity, were quite relevant in lower concentrations, mainly for the 25H-NBOH sample.

Several studies in which zebrafish embryos were exposed to different substances, malformation, oxidative stress, and DNA damage were observed (He et al., 2014; Li et al., 2020; Zhang et al., 2020, 2017). In addition, the literature suggests that many licit and illicit drugs such as cocaine, ecstasy, MDMA, opioids, benzodiazepine, and carbamazepine, sertraline, can induce DNA damage (Alvarenga et al., 2010; Barenys et al., 2009; Parolini et al., 2017; Subedi et al., 2021). -Álvarez-Alarcón et al., 2021 recently reported that the 25C-NBOMe, a chloro phenethylamine derivative, promoted alterations in the motor response stimulus as well as abnormal development in zebrafish, suggesting a teratogenic effect. There is the possibility that the effects observed in zebrafish embryos and larvae in this study were at least in part due to an overactivation of the receptors that are products of orthologous gene expression of human 5-HT receptors.

Regarding the occurrence of 5HT2A receptors, it was reported that zebrafish larvae with 5 dpf (days post-fertilization) present htr2ab [orthologous to human HTR2A (5-hydroxytryptamine receptor 2A)] expression (0.194 RPKM) very close to that determined in the head of adult females (0.215 RPKM) (BioProject: PRJEB1986, https://www.ncbi.nlm.nih.gov/gene/559806). Xing et al. (2015) showed even earlier the expression of htr2ab in embryos with only 2 dpf. In turn, Sourbron et al. (2016) showed that zebrafish larvae (7 dpf) express the orthologues of all human 5-HT receptor subtypes, including htr2ab that was effectively activated by a specific agonist and caused behavioral changes. As for the toxic effects of 25H-NBOMe

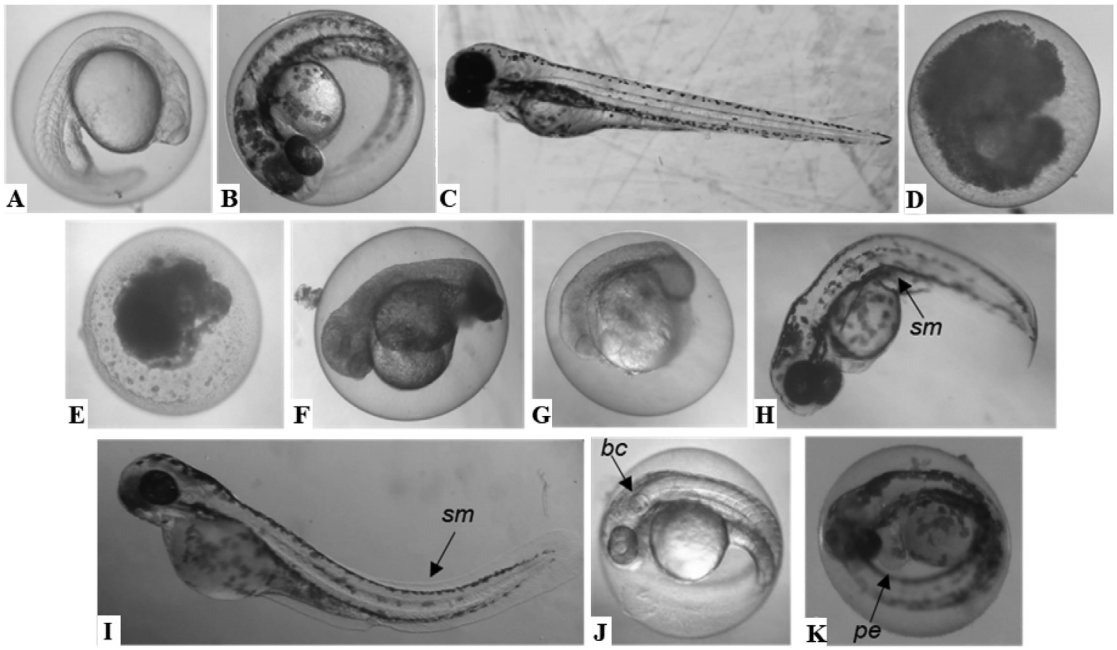

Fig. 3. Lethal and non-lethal effects were observed in zebrafish embryos and larvae (n = 20 / concentration) after exposure to increasing 25H-NBOH or 25H-NBOMe concentrations. (A), (B) and (C) Control organisms with normal development after 24, 48, and 96 h exposed only to E3 medium; (D) and (E) 24 h-old embryos coagulated exposed to 80 and 100 μg mL^{-1} of 25H-NBOH and 25H-NBOMe, respectively; (F) and (G) 48 h-old embryos with body malformation exposed to 80 and 100 μg mL^{-1} of 25H-NBOH and 25H-NBOMe, respectively; (H) and (I) 96 h-old hatched larva with spine malformation (sm) exposed to 10 and 50 μg mL^{-1} of 25H-NBOH and 25H-NBOMe, respectively; (J) 48 h-old embryo with blood clotting (bc) exposed to 50 μg mL^{-1} of 25H-NBOMe; (K) 96 h-old embryo with pericardial edema (pe) and hatching delay exposed to 100 μg mL^{-1} of 25H-NBOMe.

Table 1
Effects of 25H-NBOH and 25H-NBOMe on developmental parameters of zebrafish early stages after 96 h of exposure.

Embryotoxicological endpoints	25H-NBOH	25H-NBOMe
Otolith malformation	-[b]	100
Spine malformation	10[a]	50[a]
Egg hatching delay	20[a]	70[a]
Body malformation	80[a]	100
Pericardial edema	–	100[a]
Blood clotting	–	50[a]
Mortality (LC_{50})[c]	43 (31–60)	84 (56–123)

[a] Values are LOAEL (Lowest-observed-adverse-effect level) in μg mL^{-1}.
[b] No effects or less than 20% of embryos affected on the endpoint analysed.
[c] LC_{50} values are in mg L^{-1} followed by 95% CI between brackets.

and 25H-NBOH on zebrafish, Kawahara et al. (2017) showed that 25B-NBOMe altered the survival rate, locomotion, and induced changes in the spine of larvae with 2 dpf after treatment with 0.005, 0.5, or 5 μg mL^{-1} for 2 days. Treatment with 5-HT2A receptor antagonists prevented 25B-NBOMe-induced hypo-locomotion, death, and muscle injury. Recently, Álvarez-Alarcón et al. (2021) demonstrated that exposure of dechorionated zebrafish embryos to 25C-NBOMe for 96 h resulted in an LC_{50} of 10.76 μg mL^{-1} and a series of sublethal effects that included alterations in pigmentation patterns, growth and development rates, heart rhythm, and peripheral circulation, and ocular development. Besides these alterations, the authors reported the formation of pericardial and perivitelline edemas, deformation in the yolk and its elongation, and changes in the body's curvature. Finally, the acute toxicity test of ayahuasca drink (it contains DMT which has an affinity for serotonin receptors, mainly the 5-HT2A receptor) was performed on zebrafish embryos, at a concentration of 0 to 1000 μg mL^{-1} over 96 h of exposure. The LC_{50} of ayahuasca in zebrafish was determined to be 236.3 μg mL^{-1}. Ayahuasca exposure caused significant developmental anomalies in zebrafish embryos, mainly at the highest concentration tested, including hatching delay, loss of equilibrium, edema, and accumulation of red blood cells (Andrade et al., 2018). To the best of our knowledge, our study is the first to assess the toxic effects of NBOHs on zebrafish embryos.

As with other chemically related hallucinogens, 25H-NBOMe and 25H-NBOH could bind to serotonin receptors and, by mechanisms not yet known, trigger acute toxic effects in zebrafish embryos and larvae at the concentrations tested. A few studies demonstrate that substances of the NBOMe and NBOH class are metabolized in cytochrome P450, undergoing reactions such as *N*-alkylation, hydroxylation, and *O*-demethylation (Caspar et al., 2018; Nielsen et al., 2017). Since the present study demonstrated toxicity for 25H-NBOMe and 25H-NBOH, our results encourage further studies focused on absorption, metabolization, and elimination of NBOMes and NBOHs and their by-products in well-established experimental models in rodents, for example. It is known that many psychostimulants can cross the placenta and cause several adverse effects on fetal development (Ross et al., 2015). However, we did not find specific studies on the ability of NBOMes and NBOHs and/or their metabolites to cross the placental barrier. This is a gap that deserves more attention in further studies. In addition, our recent study has shown that other substances in this class, 25I-NBOH and 25I-NBOMe, are able to interact with the HSA biomacromolecule (de Barros et al., 2021a). Thus, we decided to study whether 25H-NBOH and 25H-NBOMe drugs have an affinity for DNA *in vitro* studies.

In vitro assays of DNA and 25H-NBOH/25H-NBOMe interaction

The interaction between the 25H-NBOH and 25H-NBOMe drugs with ctDNA (Calf thymus) was evaluated using UV–vis, molecular fluorescence, circular dichroism, and NMR techniques, as well as molecular theoretical studies. The ability to interact with DNA was assessed for both drugs since they showed toxicity against zebrafish *in vivo* assays.

Evaluating the drug interaction employing fluorescence spectroscopy

In evaluating the interaction between the drugs and ctDNA, it was observed that the ligands present an emission peak at 326 nm (λ_{ex} = 260 nm), and 25H-NBOMe presents a higher fluorescence intensity when compared to 25H-NBOH (Fig. 4A and S1a). Due to the drugs' intrinsic fluorescence, an interaction study was carried out by titrating them with ctDNA, and it was observed that there was a gradual decrease in the fluorescence intensity with the increase of nucleic acid concentration in the system (Fig. 4A and S1a). This phenomenon is related to the decrease in the free concentration of drugs in solution, resulting from the macromolecule interaction (Parveen et al., 2017).

The process of decreasing the intrinsic fluorescence of a fluorophore in the presence of a ligand is called quenching (static and dynamic). Static quenching refers to forming a non-fluorescent complex in the ground state, while dynamic quenching is a process in which the quencher diffuses, colliding with the fluorophore in the excited state without complex formation. The quenching processes can be distinguished by analyzing fluorescence data at different temperatures (Tao et al., 2015; Yang et al., 2017). Thus, we determined the quenching constant of these drugs by plotting the ratio of fluorescence intensity (F_0/F) in the presence and absence of ctDNA as a function of increasing ctDNA concentrations (Fig. 4B and S1b), according to the following equation:

$$\frac{F_0}{F} = 1 + K_{SV}[Q] = 1 + k_q \tau_0 [Q] \quad (1)$$

In which: F_0 and F are fluorescence intensities in the absence and presence of ctDNA, respectively, k_q is the diffusional bimolecular quenching rate constant, K_{SV} is the Stern-Volmer constant, [Q] the concentration of the species which acts as the quencher (ctDNA), and τ_0 is the average lifetime, typically 10^{-8} s (Silva et al., 2018).

It is possible to differentiate the quenching process in the interaction process of 25H-NBOH and 25H-NBOMe with ctDNA based on K_{SV} values at different temperatures (Table 2). Dynamic quenching depends upon diffusion; thus, the higher temperature leads to larger diffusion coefficients, and the K_{SV} increases with increasing temperature. However, the opposite is observed for static quenching since the increase in temperature decreases the stability of the complex ligand-DNA form (Yang et al., 2017). Therefore, the fluorescence quenching mechanism of 25H-NBOH and 25H-NBOMe interaction with ctDNA may be controlled by static quenching and complex formation in the ground state. The constant k_q was also used to characterize the quenching mechanism. When k_q is less than 2.0×10^{10} M^{-1} s^{-1}, the quenching is preferentially dynamic, whereas static quenching is expected for higher k_q values (Cui et al., 2015). The k_q values range from 0.75 to 2.80 $\times$ 10^{12} M^{-1} s^{-1}, being higher than the limiting diffusional constant. Therefore, static quenching is dominant, in agreement with the results of K_{SV} values (Table 2).

The non-covalent binding constant (K_b) and the number of binding sites (n) between the ligands and ctDNA were determined by spectrofluorometric titration:

$$\log\frac{F_0 - F}{F} = \log(K_b) + n\log[Q] \quad (2)$$

The interaction magnitude for the evaluated compounds has defined K_b values ranging from 90.47 to 27.00 $\times$ 10^4 M^{-1} (25H-NBOH) and 3.21 to 5.27 $\times$ 10^4 M^{-1} (25H-NBOMe). The value of n was close to the unit, indicating that the interaction stoichiometry is 1:1 (Fig. 4C and S1c, Table 2). The difference in the magnitude of K_b observed for the two substances shows that 25H-NBOH has a greater affinity for DNA, and possibly the forces involved in the interaction between the two drugs and macromolecule are different. This higher affinity may also be related to the higher toxicity observed for 25H-NBOH *in vivo* studies against zebrafish.

We calculated the interaction's thermodynamic parameters to understand the difference in the observed K_b values and relate them to different forces in the interaction process. The forces involved in the interaction process can include hydrogen bonds, van der Waals forces, hydrophobic and electrostatic interactions. Thermodynamic parameters such as the variation of free energy (ΔG), enthalpy (ΔH), and entropy (ΔS) are essential to determine the preferred type of forces which guide the interaction process. These parameters can be calculated using the K_b values at different temperatures from Van't Hoff and Gibbs free energy equations:

$$\ln(K_b) = -\frac{\Delta H}{R} \times \left(\frac{1}{T}\right) + \frac{\Delta S}{R} \quad (3)$$

$$\Delta G = \Delta H - T\Delta S \quad (4)$$

The variation of Gibbs free energy (ΔG) was negative for both drugs, so the interaction process occurs spontaneously (Table 2). However, different signs were observed for the ΔH and ΔS values. In 1981, Ross and Subramanian characterized the signal and magnitude of the thermodynamic parameters associated with the interaction process' different forces. They determined that both positive ΔH and ΔS values are associated with interactions which preferably occur by hydrophobic forces, while negative ΔH and ΔS values are related to hydrogen bonds and van der Waals forces (Ross and Subramanian, 1981). Thus, the interaction between 25H-NBOH and ctDNA preferably occurs through hydrogen bonds and van der Waals forces, whereas 25H-NBOMe preferentially interacts by hydrophobic forces. This difference

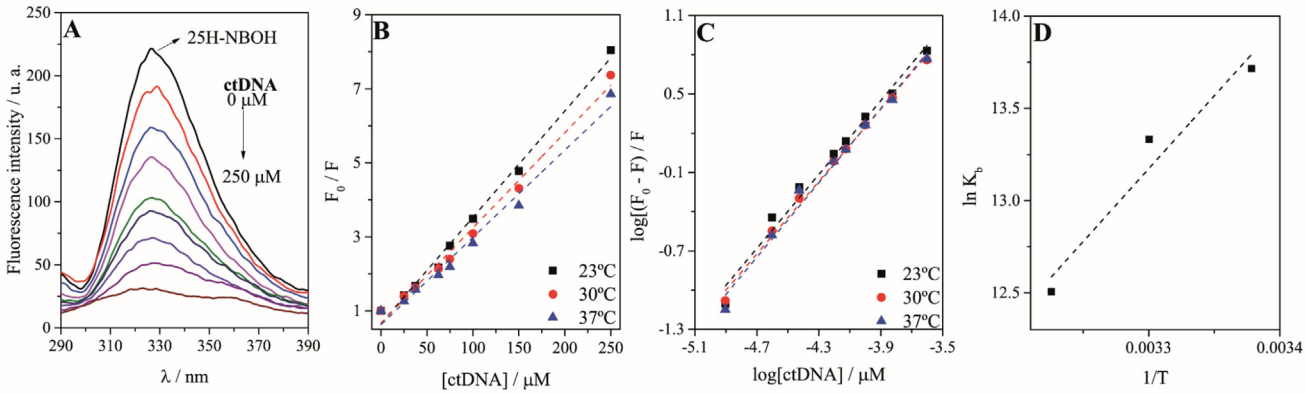

Fig. 4. (A) Fluorescence spectra of 25H-NBOH (7.5 μM) in the absence and presence of ctDNA (0–250 μM; pH 7.4, λ_{ex} = 260 nm, λ_{em} = 326 nm); (B) Stern–Volmer plots for the fluorescence quenching of 25H-NBOH by ctDNA at three different temperatures; (C) Double logarithmic curve of ctDNA quenching the fluorescence of 25H-NBOH (D) Van't Hoff curve for the 25H-NBOH-ctDNA interaction process.

Table 2
The quenching constants (K_{SV}), binding constants (K_b), number of ligand sites (n), and relative thermodynamic parameters for the interaction of 25H-NBOH and 25H-NBOMe with ctDNA at different temperatures.

Ligand	T (°C)	Binding parameters						Thermodynamics parameters		
		K_{SV} (10^4 M^{-1})	k_q (10^{12} M^{-1} s^{-1})	r	K_b (10^4 M^{-1})	r	n	ΔH (kJ mol^{-1})	ΔS (J K^{-1} mol^{-1})	ΔG (kJ mol^{-1})
25H-NBOH	23	2.80 ± 0.02	2.80	0.9893	90.47 ± 0.01	0.9920	1.41			−33.95
	30	2.57 ± 0.01	2.57	0.9948	61.69 ± 0.01	0.9975	1.39	−65.70	−107.26	−33.20
	37	2.36 ± 0.01	2.36	0.9913	27.00 ± 0.01	0.9969	1.29			−32.45
25H-NBOMe	23	0.85 ± 0.02	0.85	0.9967	3.21 ± 0.01	0.9987	1.16			−25.57
	30	0.77 ± 0.04	0.77	0.9881	4.29 ± 0.01	0.9944	1.21	+27.05	+177.76	−26.81
	37	0.75 ± 0.02	0.75	0.9964	5.27 ± 0.01	0.9947	1.23			−28.10

in the forces involved in the interaction may result from structural differences in the drugs. 25H-NBOH has a hydroxyl group, a site capable of donating and receiving hydrogen bonding, and stronger interactions than hydrophobic forces; therefore, 25H-NBOH has greater ctDNA affinity, thereby justifying the higher K_b.

Interaction studies of ctDNA with 25H-NBOH/25H-NBOMe by UV–vis

UV–vis absorption spectroscopy is one of the most straightforward and widely used techniques in assessing DNA stability and the process of interaction with ligands. Molecular absorption spectra for 25H-NBOH in the absence and presence of ctDNA are shown in Fig. S2. 25H-NBOH and ctDNA present maximum absorption wavelengths close to 258 nm; however, by adding nucleic acid to the compound solution, a displacement to longer wavelengths ($\Delta\lambda \approx 8$ nm) characterizing a hypsochromic effect occurs. These results confirm the interaction between ligand and macromolecule (Savariz et al., 2014). Thus, in general, when the ligand interacts with DNA and forms a complex, changes in the absorbance values and the band position may occur due to electronic transitions $n \rightarrow \pi^*$ and $\pi \rightarrow \pi^*$ of the ligand and $\pi \rightarrow \pi^*$ of the DNA. The spectral evaluation found that the 25H-NBOH-ctDNA complex absorbance value at the maximal wavelength ($A_{complex}$) was different from the sum of the free 25H-NBOH and free ctDNA absorbance values ($A_{ligand} + A_{ctDNA}$), evidencing that there was no additive effect of the Beer law (Savariz et al., 2014).

Furthermore, the spectrum resulting from the subtraction of the supramolecular complex spectrum (25H-NBOH-ctDNA) and the free ctDNA spectrum did not overlap the free ligand spectrum, confirming the interaction between the compound and ctDNA (Table S1). The results obtained for the 25H-NBOMe and ctDNA system were similar to those obtained for the 25H-NBOH (Fig. S2b and Table S1). Finally, this result indicates that the ligand and nucleic acid complex formation occurred in the ground state, confirming that the preferred quenching mechanism is static.

Evaluation of the ligand-ctDNA non-covalent binding mode

Ligands traditionally interact with DNA in three ways: between nitrogen base pairs (intercalation), major or minor groove, and electrostatic binding (Kashanian et al., 2012). The non-covalent binding mode between 25H-NBOH and 25H-NBOMe with ctDNA was evaluated through ionic strength effect, potassium iodide (KI), melting point, and competition assays using DNA probes with well-establishing interaction mode.

Ionic strength effect

DNA is an anionic polymer due to phosphate groups in its structure (Bi et al., 2015). The estimated pKa for 25H-NBOH and 25H-NBOMe are 10.38 and 9.11, respectively, and at physiological pH (7.40). The compounds consequently present a positive charge in the solution, and they can interact with the external phosphate backbone of nucleic acid electrostatically. The ionic strength effect on the interaction between 25H-NBOH and 25H-NBOMe with ctDNA was evaluated by adding different NaCl concentrations due to the weakening of the electrostatic attraction between small molecules and the DNA surface adding Na^+ (Chuan et al., 2005). The results showed that the addition of NaCl had little effect on the K_b (Fig. S3), suggesting that the electrostatic binding of 25H-NBOH and 25H-NBOMe to ctDNA could be neglected.

Potassium iodide assay (KI)

Potassium iodide assay can be used to study non-covalent DNA binding modes since iodide ions cause quenching in the fluorescent compound if they are accessible. When a ligand interacts via intercalation, the DNA double helix protects the compound from the quencher's action, and thus the magnitude of the K_{SV} value is less than the free ligand (Huo et al., 2012). The Stern-Volmer constant values in the absence and presence of the ctDNA were used as a comparison parameter. The K_{SV} was calculated according to Eq. (1), in which [Q] is the KI concentration (Fig. 5A and S4a).

The ligands' K_{SV} values were slightly lower in the presence of ctDNA, being 1.20 and 1.16 timeless for 25H-NBOH and 25H-NBOMe, respectively, comparing free ligands and in the presence of ctDNA. These results suggest that the ligands do not bind to DNA via intercalation mode and are therefore not protected by nitrogenous bases, as K_{SV} values for intercalated drug molecules within DNA base pairs are expected to be 5–7 times less compared to the free-drug (Kundu and Chattopadhyay, 2017). Thus, the probable interaction mode between the 25H-NBOH and 25H-NBOMe drugs with DNA binds in the groove.

Thermal denaturation studies

Determining the melting temperature (T_m) of DNA is an important technique that can elucidate small compounds' binding mode to the double strand of DNA. T_m is the temperature at which half of the DNA in a solution converts into a single-stranded form, and changes in the T_m value can reflect changes in the DNA's stability. Intercalation of small molecules in the duplex increases their stability and, in turn, increases the melting temperature by about 5–8 °C. On the other hand, the non-intercalative compounds cause no evident variation in T_m (Ahmad et al., 2016). Thus, the T_m of ctDNA was determined by monitoring ctDNA absorbance (260 nm) in the absence and presence of 25H-NBOH or 25H-NBOMe at different temperatures. The single-stranded fraction (f_{ss}) was calculated by:

$$f_{ss} = \frac{A - A_0}{A_f - A_0} \quad (5)$$

In which: A is the absorbance at T temperature, while A_0 and A_f are the absorbances at the initial and final temperatures. The T_m (f_{ss} = 0.5) of ctDNA was 85.3 °C (Fig. 5B and S4b); however, there was a decrease in this value upon the addition of 25H-NBOH and 25H-NBOMe. The T_m in the presence of 20 and 100 μM of 25H-NBOH was 83.2 °C (ΔT = -2.1) and 67 °C (ΔT = -18.3), respectively, whereas there was also a decrease in T_m for 25H-NBOMe in the same concentration, but to a lesser magnitude, being 80.7 °C (ΔT = -4.6)

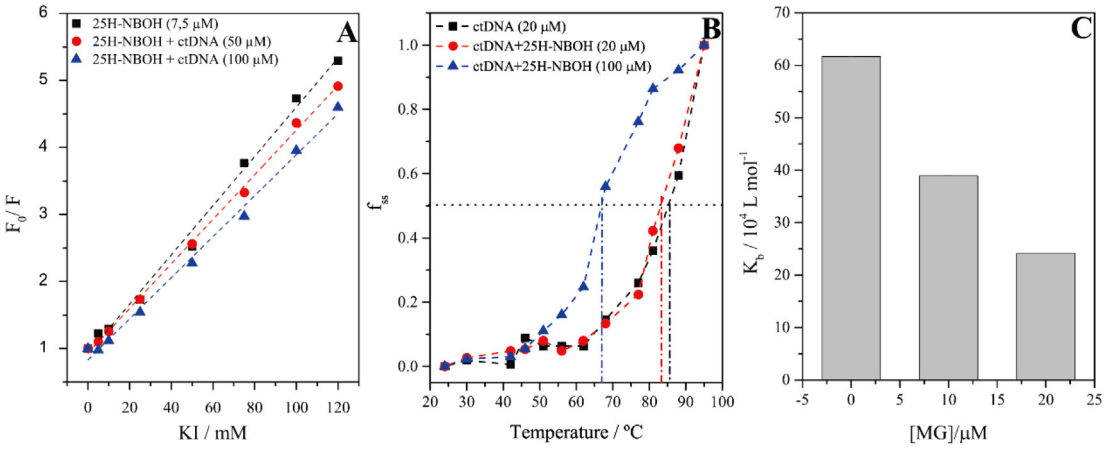

Fig. 5. (A) Stern–Volmer plots for the quenching of 25H-NBOH by KI in the absence and presence of ctDNA. (B) Melting curves of ctDNA in the absence and presence of 25H-NBOH at pH 7.4. (C) Binding constant values (K_b) of 25H-NBOH interaction with ctDNA in the absence and presence of MG.

and 77.9 °C (ΔT = -7.4). The literature indicates that reduction in T_m is characteristic of molecules capable of establishing hydrogen bonds with nucleotides (Bathaie et al., 2010), so the decreased T_m results may be associated with the fact that both substances have groups capable of forming a hydrogen bond. The greater magnitude of the decrease observed for 25H-NBOH may be associated with the presence of the structure's hydroxyl group. Finally, it was evident that there was atypical behavior concerning the evaluated compounds and the interaction mode with DNA.

Competitive displacement assay

In the literature, a displacement experiment of fluorescent probes with a well-established binding mode was carried out to confirm the non-covalent binding mode. Thus, ethidium bromide (EB), acridine orange (AO), thiazole orange (TO), and berberine (BB) probes were used for the intercalative binding mode, while DAPI and Hoechst (HO) were used for the minor groove binding mode (Tao et al., 2016). These probes show high fluorescence intensity upon binding to DNA, and the capacity of 25H-NBOH and 25H-NBOMe to replace them from their binding sites was evaluated, causing a decrease in the fluorescence intensity. As previous experiments suggested that the binding mode is not by intercalation, it was already expected that the ligands would not displace the EB, AO, TO, and BB (Fig. S5). However, no reductions in fluorescence intensity was observed for DAPI or HO probes, showing that the binding mode of 25H-NBOH and 25H-NBOMe with DNA does not occur by intercalation or in the minor groove.

The results suggest that 25H-NBOH and 25H-NBOMe possibly bind to DNA by a major groove; however, commercial probes and a well-established binding mode for a major groove were not commonly found. Few studies in the literature show that the methyl green (MG) dye has an affinity for the DNA major groove, so it was used to confirm our binding mode hypothesis (Kim and Nordén, 1993; Prieto et al., 2014). Due to the low fluoresce intensity complex (MG-DNA), MG was used as a competitor of the binding site and not as a fluorescent probe. Thus, it was evaluated how the presence of MG in the titration of 25H-NBOH and 25H-NBOMe with ctDNA would affect the binding constant's values. A decrease in the K_b value by 60 and 80% were obtained for 25H-NBOH and 25H-NBOMe, respectively (Fig. 5C and S4c). These results suggest that the interaction between drugs and ctDNA is unfavorable in the presence of MG, probably due to competition for the same binding site; thus, based on our results, the 25H-NBOH and 25H-NBOMe drugs non-classically interact in the major DNA groove.

Circular dichroism spectral studies (CD)

Circular dichroism (CD) was used to monitor possible conformational changes in the DNA structure. Two characteristic B-DNA bands are observed in CD spectra of ctDNA in the absence and presence of 25H-NBOH or 25H-NBOMe (Fig. 6), a negative band at 245 nm associated with the double helix structure in the right direction, and the band at 275 nm refers to the stacking of nitrogenous bases (Yang et al., 2017).

Conformational changes in DNA structure can be assessed by increasing or decreasing the intensity of these bands. The intercalation of small compounds usually changes the DNA CD spectra, enhancing both CD bands' intensities. However, ligand groove binding displays low or no perturbation in absorption bands (Xie et al., 2015). Corroborating with the major groove binding mode, the interaction of 25H-NBOH and 25H-NBOMe with ctDNA did not cause drastic changes in the absorption bands on CD spectra. No significant change in band intensity at 245 nm (Fig. 6) shows that the drug interaction does not affect the double helix structure in the right direction. However, a decrease in the intensity of the positive band at 275 nm was observed. This result suggests an increase in the base stacking degree of ctDNA, inducing a conformational change of ctDNA to a more compact structure (Wang and Yang, 2009).

NMR studies

NMR is a powerful technique for probing and understanding binding between a small molecule and macromolecules by monitoring the ligand or macromolecule (Yang et al., 2017). However, monitoring macromolecule chemical shifts are challenging to analyze without isotope-labeling, making the study of the ligands more appreciable since it provides more simplified and resolved NMR spectra. In particular, ^{1}H NMR spectra could help determine the binding epitope, which characterizes the ligand's hydrogens closer to the macromolecule upon binding (Figueiredo and Marsaioli, 2007; Viegas et al., 2011). Intercalation, partially intercalated binding, and groove binding types of ligand-DNA interaction modes are differentiated by ^{1}H NMR signals based on changing line widths and chemical shifts. Thus, the intercalation of ligands into base pairs of DNA results in complete line broadening of the ^{1}H NMR signal, while line broadening and an up-field shift are observed in partially intercalated molecules (Sartorius and Schneider, 1997). However, strong line broadening and up-field shift of the ^{1}H NMR signal is not observed for molecules that bind to DNA grooves (Yang et al., 2017).

The binding epitope was determined from the variation of the chemical shift of the hydrogen signals of the ligands in the absence

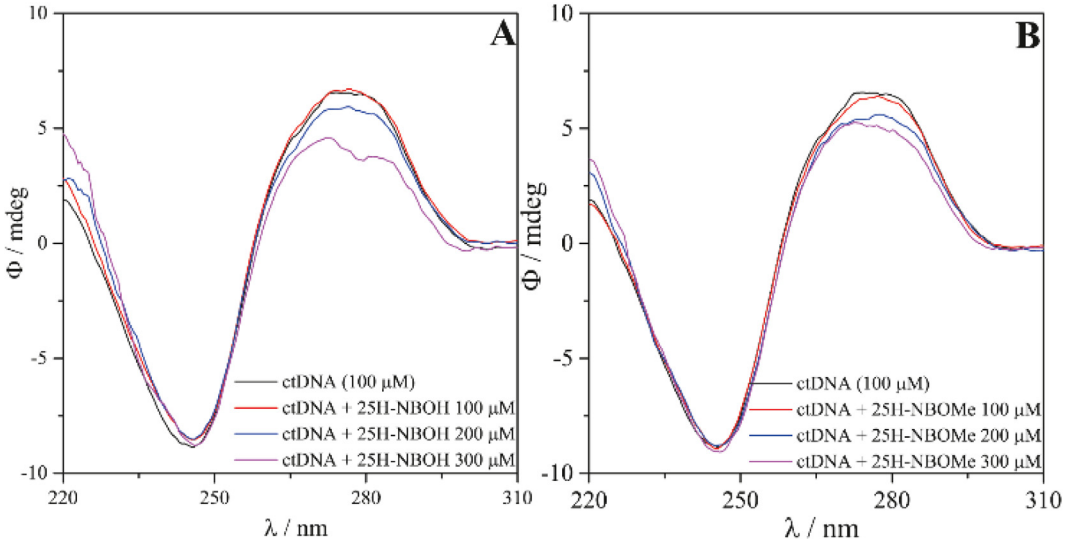

Fig. 6. CD spectra of ctDNA in the presence of increasing amounts of (A) 25H-NBOH and (B) 25H-NBOMe at pH 7.4 and 25 °C.

and presence of ctDNA, and the Δδ ($\Delta\delta = \delta_{\text{free ligand}} - \delta_{\text{complex}}$) was subsequently calculated. Variations in the hydrogen signals' chemical shift were observed for all excesses of ctDNA, with positive values of $\Delta\delta$, indicating a downfield in the NMR signals (Tables S2 and S3) and a little line broadening signals. ^{1}H NMR spectra of the ligands in the absence and presence of DNA were recorded (Figs. S6 and S7). For 25H-NBOH and 25H-NBOMe (Fig. 7), the signals referring to the H8′, H9, and H10 hydrogens were downfield in the presence of the ctDNA; these hydrogens are neighbors to the amino group, showing that the presence of this group influences the interaction with DNA. The signs of the aromatic hydrogens of ring B (3′, 4′, 5′ and 6′) of the 25H-NBOH showed a more pronounced downfield compared to 25H-NBOMe (Tables S2 and S3), which may be the result of the presence of the hydroxyl group in 25H-NBOH which influences the interaction process with DNA. The slight line broadening of the signals and the lack of upfield of the NMR signals are consistent for molecules that interact in the DNA groove (Yang et al., 2017).

Molecular modeling (MD) interaction studies

Docking and MD simulations were carried out to obtain detailed information about the interactions of 25H-NBOH and 25H-NBOMe with DNA to corroborate spectroscopic results. It was initially observed from the docking studies that both drugs presented affinity to the major DNA groove (Fig. 8A and D). Then, both the complexes obtained after docking procedures were subjected to an MD simulation to understand the mechanism of interactions with DNA better, and after 100 ns, we observed that both drugs remained in a major groove (Fig. 8B and 8E). Hence, it can be concluded that *in silico* studies corroborated with competitive displacement assay, in which both ligands showed a reduction in the K_b values, probably due to competition with the MG probe. The Root Mean Square Deviation (RMSD) plots of the DNA backbone during the MD simulations (Fig. 8C and F), the averages for 25H-NBOH-DNA and 25H-NBOMe-DNA complexes ranged from 0.1 to 0.3 nm. Finally, both MD simulations showed that the ligand-DNA complexes remained stable until the end, corroborating with the higher DNA affinity of the drugs observed in experimental data.

The most prevalent conformations during MD simulations for 25H-NBOH and 25H-NBOMe were archived (Fig S8). It was observed that the amino group acts as a hydrogen donor in conventional H-bond interactions with the guanine 4 (DG4) and adenine 18 (DA18) base pairs for 25H-NBOH and 25H-NBOMe, respectively. Moreover, two other hydrogen bond interactions were observed for the 25H-NBOH drug between free hydroxyl and methoxy groups with cytosine bases

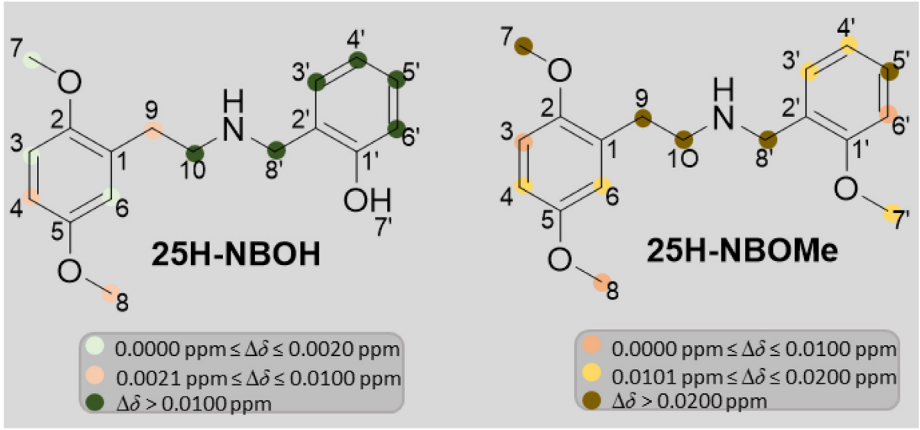

Fig. 7. Proposed 25H-NBOH and 25H-NBOMe epitopes based on ^{1}H NMR chemical variation (Δδ) in the presence of HSA.

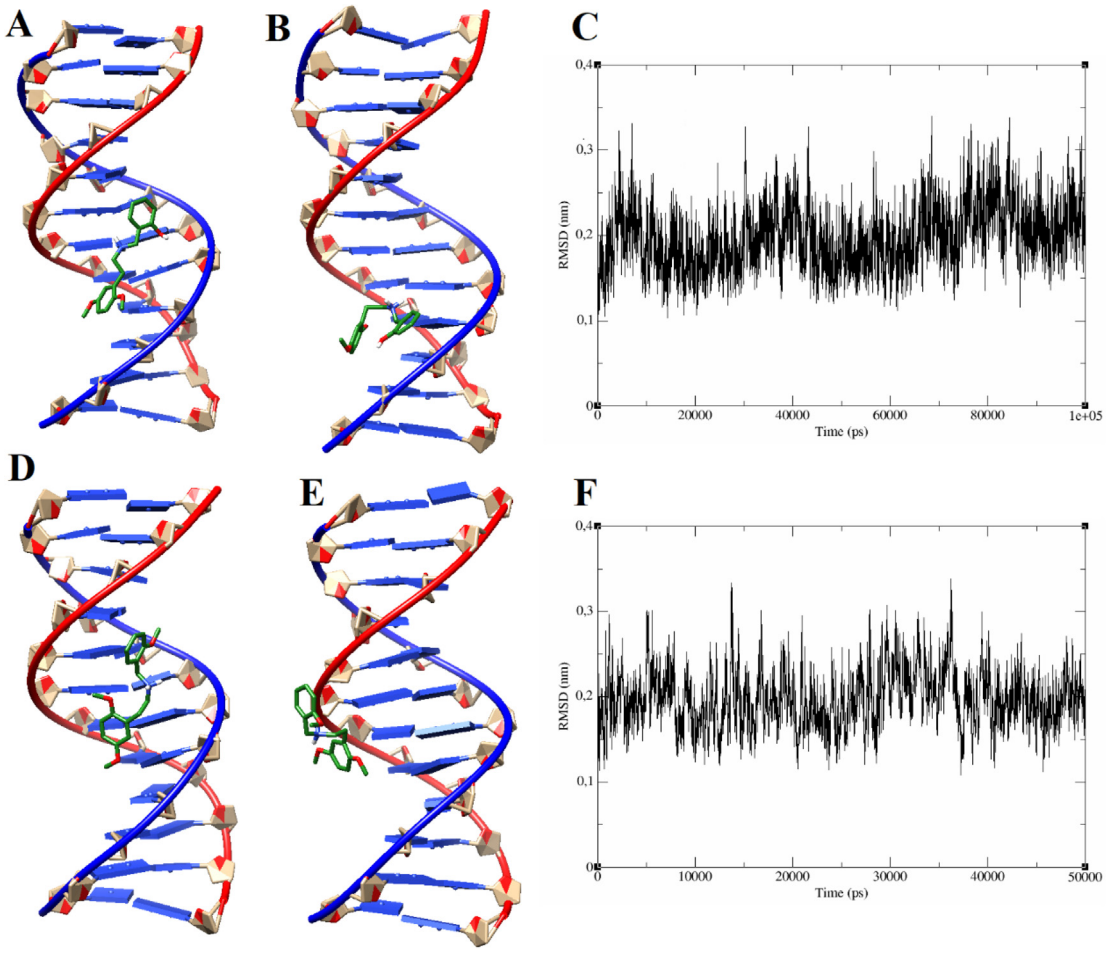

Fig. 8. Representation of the best docking conformations for (A) 25H-NBOH and (D) 25H-NBOMe; (B) and (E) drugs complexed with DNA after MD simulations; (C) and (F) show the RMSD plot for the DNA backbone during each MD simulation.

3 (DC3) and 21 (DC21). These additional interactions follow this compound's spectroscopic results and might explain their greater affinity for ctDNA, higher K_b value, and *in vivo* toxicity than the methylated analog.

Conclusion

In this work, the zebrafish embryos model showed that the 25H-NBOH and 25H-NBOMe are highly toxic *in vivo*, causing embryo malformation and lethal effects ($LC_{50} \leq 83$ μg mL^{-1}). We also evaluated the interaction of these drugs with ctDNA exploring biophysical strategies since the toxic effects observed *in vivo* may be related to the interaction of drugs with DNA. Therefore, 25H-NBOH and 25H-NBOMe are capable of non-classically interacting in the major DNA groove. The spectroscopic studies showed that 25H-NBOH preferably interacts by van der Waals forces and hydrogen bonds. The ability of these substances to bind to DNA can integrate the mechanisms of toxicity and be related to the adverse effects observed in zebrafish. Since the zebrafish embryo model has risen as a gold standard in developmental toxicity studies, high homology genome with the human and the conservation of toxicity pathways, it is to be assumed that the toxic effects of the studied hallucinogens may be represented in other vertebrates, including in humans. However, it is too early to state that a man who uses 25H-NBOMe and 25H-NBOH may have his liver, for example, damaged by the toxic effects of these substances or that a pregnant woman will have adverse effects on the embryo or fetus in development. Absorption, metabolization, and elimination studies of these substances and their metabolites at realistic concentrations in cell culture models and vertebrates (zebrafish larvae and rodents) still need to be carried out better to understand the risks and toxicity mechanisms of these hallucinogens.

CRediT authorship contribution statement

AF and JCCS contributed with the conceptualization, funding acquisition, project administration, supervision, validation, formal analysis, writing – original draft and writing – review & editing the work. WAB contributed with the conceptualization, data curation, formal analysis, writing – original draft and writing – review & editing the work. IMF and CSN contributed with the conceptualization, data curation, formal analysis, writing – original draft and writing – review & editing the work. DF, JACR and LV contributed with the conceptualization, formal analysis, writing – original draft and writing – review & editing the work. TMA and IJSN contributed with the conceptualization, software, formal analysis, writing – original draft and writing – review & editing the work.

Declaration of Competing Interest

The authors declare that they have no known competing financial interests or personal relationships that could have appeared to influence the work reported in this paper.

Acknowledgments

This study was funded by the Conselho Nacional de Desenvolvimento Científico e Tecnológico (CNPq/Brazil - Grant #429121/2018-0), Coordenação de Aperfeiçoamento de Pessoal de Nível Superior (CAPES/Brazil - Finance Code 001 - Grant # 88881.516313/2020-01), Fundação de Amparo à Pesquisa do Estado de Alagoas (FAPEAL/Brazil – Grant # 60030 000863/2016), and Fundação de Amparo à Pesquisa do Estado de Minas Gerais (FAPEMIG/Brazil; Grant # RED-00042-16). ADF and JCCS are recipient of research fellowship from CNPq/Brazil.

Appendix A. Supplementary data

Supplementary data to this article can be found online at https://doi.org/10.1016/j.crtox.2021.11.002.

References

Ahmad, I., Ahmad, A., Ahmad, M., 2016. Binding properties of pendimethalin herbicide to DNA: multispectroscopic and molecular docking approaches. Phys. Chem. Chem. Phys. 18 (9), 6476–6485. https://doi.org/10.1039/C5CP07351K.

Alvarenga, T.A., Andersen, M.L., Ribeiro, D.A., Araujo, P., Hirotsu, C., Costa, J.L., Battisti, M.C., Tufik, S., 2010. Single exposure to cocaine or ecstasy induces DNA damage in brain and other organs of mice. Addict. Biol. 15, 96–99. https://doi.org/10.1111/j.1369-1600.2009.00179.x.

Álvarez-Alarcón, N., Osorio-Méndez, J.J., Ayala-Fajardo, A., Garzón-Méndez, W.F., Garavito-Aguilar, Z.V., 2021. Zebrafish and Artemia salina in vivo evaluation of the recreational 25C-NBOMe drug demonstrates its high toxicity. Toxicol. Reports 8, 315–323. https://doi.org/10.1016/j.toxrep.2021.01.010.

Andreasen, M.F., Telving, R., Rosendal, I., Eg, M.B., Hasselstrøm, J.B., Andersen, L.V., 2015. A fatal poisoning involving 25C-NBOMe. Forensic Sci. Int. 251, e1–e8. https://doi.org/10.1016/j.forsciint.2015.03.012.

Andrade, T.S., de Oliveira, R., da Silva, M.L., Von Zuben, M.V., Grisolia, C.K., Domingues, I., Caldas, E.D., Pic-Taylor, A., 2018. Exposure to ayahuasca induces developmental and behavioral alterations on early life stages of zebrafish. Chem Biol Interact. 25 (293), 133–140. https://doi.org/10.1016/j.cbi.2018.08.001.

Arantes, L.C., Júnior, E.F., de Souza, L.F., Cardoso, A.C., Alcântara, T.L.F., Lião, L.M., Machado, Y., Lordeiro, R.A., Neto, J.C., Andrade, A.F.B., 2017. 25I-NBOH: a new potent serotonin 5-HT2Areceptor agonist identified in blotter paper seizures in Brazil. Forensic Toxicol. 35 (2), 408–414. https://doi.org/10.1007/s11419-017-0357-x.

Barenys, M., Macia, N., Camps, L., de Lapuente, J., Gomez-Catalan, J., Gonzalez-Linares, J., Borras, M., Rodamilans, M., Llobet, J.M., 2009. Chronic exposure to MDMA (ecstasy) increases DNA damage in sperm and alters testes histopathology in male rats. Toxicol. Lett. 191 (1), 40–46. https://doi.org/10.1016/j.toxlet.2009.08.002.

Bathaie, S.Z., Nikfarjam, L., Rahmanpour, R., Moosavi-Movahedi, A.A., 2010. Spectroscopic studies of the interaction of aspirin and its important metabolite, salicylate ion, with DNA, A·T and G·C rich sequences. Spectrochim. Acta - Part A Mol Biomol. Spectrosc. 77 (5), 1077–1083. https://doi.org/10.1016/j.saa.2010.08.078.

Bersani, F.S., Corazza, O., Albano, G., Valeriani, G., Santacroce, R., Bolzan Mariotti Posocco, F., Cinosi, E., Simonato, P., Martinotti, G., Bersani, G., Schifano, F., 2014. 25C-NBOMe: Preliminary Data on Pharmacology, Psychoactive Effects, and Toxicity of a New Potent and Dangerous Hallucinogenic Drug. Biomed Res. Int. 2014, 1–6. https://doi.org/10.1155/2014/734749.

Bi, S., Zhao, T., Wang, Y., Zhou, H., Pang, B., Gu, T., 2015. Binding studies of terbutaline sulfate to calf thymus DNA using multispectroscopic and molecular docking techniques. Spectrochim. Acta Part A Mol. Biomol. Spectrosc. 150, 921–927. https://doi.org/10.1016/j.saa.2015.06.042.

Braga, T.C., Silva, T.F., Maciel, T.M.S., da Silva, E.C.D., da Silva-Júnior, E.F., Modolo, L. V., Figueiredo, I.M., Santos, J.C.C., de Aquino, T.M., de Fátima, Ă., 2019. Ionic liquid-assisted synthesis of dihydropyrimidin(thi)one Biginelli adducts and investigation of their mechanism of urease inhibition. New J. Chem. 43 (38), 15187–15200. https://doi.org/10.1039/C9NJ03556G.

Braida, D., Limonta, V., Pegorini, S., Zani, A., Guerini-Rocco, C., Gori, E., Sala, M., 2007. Hallucinatory and rewarding effect of salvinorin A in zebrafish: κ-opioid and CB1-cannabinoid receptor involvement. Psychopharmacology (Berl). 190 (4), 441–448. https://doi.org/10.1007/s00213-006-0639-1.

Cachat, J., Canavello, P., Elegante, M., Bartels, B., Hart, P., Bergner, C., Egan, R., Duncan, A., Tien, D., Chung, A., Wong, K., Goodspeed, J., Tan, J., Grimes, C., Elkhayat, S., Suciu, C., Rosenberg, M., Chung, K.M., Kadri, F., Roy, S., Gaikwad, S., Stewart, A., Zapolsky, I., Gilder, T., Mohnot, S., Beeson, E., Amri, H., Zukowska, Z., Soignier, R.D., Kalueff, A.V., 2010. Modeling withdrawal syndrome in zebrafish. Behav. Brain Res. 208 (2), 371–376. https://doi.org/10.1016/j.bbr.2009.12.004.

Cassar, S., Adatto, I., Freeman, J.L., Gamse, J.T., Iturria, I., Lawrence, C., Muriana, A., Peterson, R.T., Van Cruchten, S., Zon, L.I., 2020. Use of Zebrafish in Drug Discovery Toxicology. Chem. Res. Toxicol. 33 (1), 95–118. https://doi.org/10.1021/acs.chemrestox.9b00335.

Caspar, A.T., Meyer, M.R., Maurer, H.H., 2018. Human cytochrome P450 kinetic studies on six N-2-methoxybenzyl (NBOMe)-derived new psychoactive substances using the substrate depletion approach. Toxicol. Lett. 285, 1–8. https://doi.org/10.1016/j.toxlet.2017.12.017.

Chuan, D., Yu-xia, W., Yan-li, W., 2005. Study on the interaction between methylene violet and calf thymus DNA by molecular spectroscopy. J. Photochem. Photobiol. A Chem. 174 (1), 15–22. https://doi.org/10.1016/j.jphotochem.2005.02.007.

Corazza, O., Assi, S., Simonato, P., Corkery, J., Bersani, F.S., Demetrovics, Z., Stair, J., Fergus, S., Pezzolesi, C., Pasinetti, M., Deluca, P., Drummond, C., Davey, Z., Blaszko, U., Moskalewicz, J., Mervo, B., Furia, L.D., Farre, M., Flesland, L., Pisarska, A., Shapiro, H., Siemann, H., Skutle, A., Sferrazza, E., Torrens, M., Sambola, F., van der Kreeft, P., Scherbaum, N., Schifano, F., 2013. Promoting innovation and excellence to face the rapid diffusion of Novel Psychoactive Substances in the EU: the outcomes of the ReDNet project. Hum. Psychopharmacol. Clin. Exp. 28 (4), 317–323. https://doi.org/10.1002/hup.2299.

Csizmadia, P., 1999. MarvinSketch and MarvinView: Molecule Applets for the World Wide Web, in: Proceedings of The 3rd International Electronic Conference on Synthetic Organic Chemistry. MDPI, Basel, Switzerland, p. 1775. https://doi.org/10.3390/ecsoc-3-01775

Cui, F., Niu, X., Li, L., Zhang, P., Zhang, G., 2015. Interaction of Anthracycline 3′-azido-epirubicin with Calf Thymus DNA via Spectral and Molecular Modeling Techniques. J. Fluoresc. 25 (4), 1109–1115. https://doi.org/10.1007/s10895-015-1601-6.

Dai, Y.-J., Jia, Y.-F., Chen, N.a., Bian, W.-P., Li, Q.-K., Ma, Y.-B., Chen, Y.-L., Pei, D.-S., 2014. Zebrafish as a model system to study toxicology. Environ. Toxicol. Chem. 33 (1), 11–17. https://doi.org/10.1002/etc.2406.

de Barros, W.A., Silva, M.d.M., Dantas, M.D.d.A., Santos, J.C.C., Figueiredo, I.M., Chaves, O.A., Sant'Anna, C.M.R., de Fátima, Ă., 2021a. Recreational drugs 25I-NBOH and 25I-NBOMe bind to both Sudlow's sites I and II of Human Serum Albumin (HSA): Biophysical and molecular modeling studies. New J. Chem. 45 (29), 13158–13167. https://doi.org/10.1039/D1NJ00806D.

de Barros, W.A., Queiroz, M.P., da Silva Neto, L., Borges, G.M., Martins, F.T., de Fátima, Ă., 2021b. Synthesis of 25X-BOMes and 25X-NBOHs (X = H, I, Br) for pharmacological studies and as reference standards for forensic purposes. Tetrahedron Lett. 152804. https://doi.org/10.1016/j.tetlet.2020.152804.

Dishotsky, N.I., Loughman, W.D., Mogar, R.E., Lipscomb, W.R., 1971. LSD and genetic damage. Science (80-. 172 (3982), 431–440.

Félix, L.M., Serafim, C., Martins, M.J., Valentim, A.M., Antunes, L.M., Matos, M., Coimbra, A.M., 2017. Morphological and behavioral responses of zebrafish after 24 h of ketamine embryonic exposure. Toxicol. Appl. Pharmacol. 321, 27–36. https://doi.org/10.1016/j.taap.2017.02.013.

Figueiredo, I.M., Marsaioli, A.J., 2007. Mapeamento das interações proteína-ligante através de técnicas de RMN de ^{1}H utilizando detecção do ligante. Quim. Nova 30, 1597–1605. https://doi.org/10.1590/S0100-40422007000700019.

Finney, D.J., 1971. Probit Analysis. Cambridge University Press, New York.

He, X., Aker, W.G., Hwang, H.-M., 2014. An in vivo study on the photo-enhanced toxicities of S-doped TiO 2 nanoparticles to zebrafish embryos (Danio rerio) in terms of malformation, mortality, rheotaxis dysfunction, and DNA damage. Nanotoxicology 8 (sup1), 185–195. https://doi.org/10.3109/17435390.2013.874050.

Huo, R., Xu, G., Jiang, X., Ge, Y., Xue, Z., Cui, F., 2012. Calf thymus DNA binding studies of the new neodymium-naproxen complex. J. Biochem. Mol. Toxicol. 26 (5), 193–198. https://doi.org/10.1002/jbt.v26.510.1002/jbt.21401.

Jih-Heng, L., Lih-Fang, L., 1998. Genetic toxicology of abused drugs. Mutagenesis 13, 557–565.

Kashanian, S., Javanmardi, S., Chitsazan, A., Paknejad, M., Omidfar, K., 2012. Fluorometric study of fluoxetine DNA binding. J. Photochem. Photobiol. B Biol. 113, 1–6. https://doi.org/10.1016/j.jphotobiol.2012.04.002.

Kawahara, G., Maeda, H., Kikura-Hanajiri, R., Yoshida, K.I., Hayashi, Y.K., 2017. The psychoactive drug 25B-NBOMe recapitulates rhabdomyolysis in zebrafish larvae. Forensic Toxicol. 35 (2), 369–375. https://doi.org/10.1007/s11419-017-0366-9.

Keshari, V., Adeeb, B., Simmons, A.E., Simmons, T.W., Diep, C.Q., 2016. Zebrafish as a model to assess the teratogenic potential of nitrite. J. Vis. Exp. e53615. https://doi.org/10.3791/53615.

Kily, L.J.M., Cowe, Y.C.M., Hussain, O., Patel, S., McElwaine, S., Cotter, F.E., Brennan, C. H., 2008. Gene expression changes in a zebrafish model of drug dependency suggest conservation of neuro-adaptation pathways. J. Exp. Biol. 211, 1623–1634. https://doi.org/10.1242/jeb.014399.

Kim, S.K., Nordén, B., 1993. Methyl green. A DNA major-groove binding drug. FEBS Lett. 315, 61–64. https://doi.org/10.1016/0014-5793(93)81133-K.

Ko, S.-K., Jin, H., Jung, D.-W., Tian, X., Shin, I., 2009. Cardiosulfa, a Small Molecule that Induces Abnormal Heart Development in Zebrafish, and Its Biological Implications. Angew. Chemie Int. Ed. 48 (42), 7809–7812. https://doi.org/10.1002/anie.v48:4210.1002/anie.200902370.

Kristofic, J.J., Chmiel, J.D., Jackson, G.F., Vorce, S.P., Holler, J.M., Robinson, S.L., Bosy, T.Z., 2016. Detection of 25C-NBOMe in three related cases. J. Anal. Toxicol. 40 (6), 466–472. https://doi.org/10.1093/jat/bkw035.

Kueppers, V.B., Cooke, C.T., 2015. 25I-NBOMe related death in Australia: A case report. Forensic Sci. Int. 249, e15–e18. https://doi.org/10.1016/j.forsciint.2015.02.010.

Kundu, P., Chattopadhyay, N., 2017. Interaction of a bioactive pyrazole derivative with calf thymus DNA: Deciphering the mode of binding by multi-spectroscopic and molecular docking investigations. J. Photochem. Photobiol. B Biol. 173, 485–492. https://doi.org/10.1016/j.jphotobiol.2017.06.022.

Larson, A., Bammer, G., 1996. Why? Who? How? Estimating numbers of illicit drug users: lessons from a case study from the Australian Capital Territory. Aust. N. Z. J. Public Health 20, 493–499.

Lawn, W., Barratt, M., Williams, M., Horne, A., Winstock, A., 2014. The NBOMe hallucinogenic drug series: Patterns of use, characteristics of users and self-reported

effects in a large international sample. J. Psychopharmacol. 28 (8), 780–788. https://doi.org/10.1177/0269881114523866.
Li, W., Zhu, L., Du, Z., Li, B., Wang, J., Wang, J., Zhang, C., Zhu, L., 2020. Acute toxicity, oxidative stress and DNA damage of three task-specific ionic liquids ([C2NH2MIm]BF4, [MOEMIm]BF4, and [HOEMIm]BF4) to zebrafish (Danio rerio). Chemosphere 249, 126119. https://doi.org/10.1016/j.chemosphere.2020.126119.
Lowe, L.M., Peterson, B.L., Couper, F.J., 2015. A Case Review of the First Analytically Confirmed 25I-NBOMe-Related Death in Washington State. J. Anal. Toxicol. 39 (8), 668–671. https://doi.org/10.1093/jat/bkv092.
Lozano Untiveros, K., da Silva, E.G., de Abreu, F.C., da Silva-Júnior, E.F., de Araújo-Junior, J.X., Mendoça de Aquino, T., Armas, S.M., de Moura, R.O., Mendonça-Junior, F.J.B., Serafim, V.L., Chumbimuni-Torres, K., 2019. An electrochemical biosensor based on Hairpin-DNA modified gold electrode for detection of DNA damage by a hybrid cancer drug intercalation. Biosens. Bioelectron. 133, 160–168. https://doi.org/10.1016/j.bios.2019.02.071.
Machado, Y., Coelho Neto, J., Lordeiro, R.A., Alves, R.B., Piccin, E., 2020. Identification of new NBOH drugs in seized blotter papers: 25B-NBOH, 25C-NBOH, and 25E-NBOH. Forensic Toxicol. 38 (1), 203–215. https://doi.org/10.1007/s11419-019-00509-7.
Malinina, L., Soler-López, M., Aymamí, J., Subirana, J.A., 2002. Intercalation of an Acridine−Peptide Drug in an AA/TT Base Step in the Crystal Structure of [d(CGCGAATTCGCG)] 2 with Six Duplexes and Seven Mg 2+ Ions in the Asymmetric Unit †. Biochemistry 41 (30), 9341–9348. https://doi.org/10.1021/bi020135c.
Mathur, P., Guo, S.u., 2010. Use of zebrafish as a model to understand mechanisms of addiction and complex neurobehavioral phenotypes. Neurobiol. Dis. 40 (1), 66–72. https://doi.org/10.1016/j.nbd.2010.05.016.
McGrath, P., Li, C.-Q., 2008. Zebrafish: a predictive model for assessing drug-induced toxicity. Drug Discov. Today 13 (9-10), 394–401. https://doi.org/10.1016/j.drudis.2008.03.002.
Mersereau, E., Boyle, C., Poitra, S., Espinoza, A., Seiler, J., Longie, R., Delvo, L., Szarkowski, M., Maliske, J., Chalmers, S., Darland, D., Darland, T., 2016. Longitudinal Effects of Embryonic Exposure to Cocaine on Morphology, Cardiovascular Physiology, and Behavior in Zebrafish. Int. J. Mol. Sci. 17, 847–865. https://doi.org/10.3390/ijms17060847.
Miller, M.A., Bershad, A.K., De Wit, H., 2015. Drug effects on responses to emotional facial expressions: Recent findings. Behav. Pharmacol. 26, 571–579. https://doi.org/10.1097/FBP.0000000000000164.
Morini, L., Bernini, M., Vezzoli, S., Restori, M., Moretti, M., Crenna, S., Papa, P., Locatelli, C., Osculati, A.M.M., Vignali, C., Groppi, A., 2017. Death after 25C-NBOMe and 25H-NBOMe consumption. Forensic Sci. Int. 279, e1–e6. https://doi.org/10.1016/j.forsciint.2017.08.028.
Neese, F., 2012. The ORCA program system. WIREs Comput. Mol. Sci. 2 (1), 73–78. https://doi.org/10.1002/wcms.v2.110.1002/wcms.81.
Nichols, D.E., Grob, C.S., 2018. Is LSD toxic? Forensic Sci. Int. 284, 141–145. https://doi.org/10.1016/j.forsciint.2018.01.006.
Nielsen, L.M., Holm, N.B., Leth-Petersen, S., Kristensen, J.L., Olsen, L., Linnet, K., 2017. Characterization of the hepatic cytochrome P450 enzymes involved in the metabolism of 25I-NBOMe and 25I-NBOH. Drug Test. Anal. 9 (5), 671–679. https://doi.org/10.1002/dta.2031.
Ninnemann, A., Stuart, G.L., 2013. The NBOMe Series: A Novel, Dangerous Group of Hallucinogenic Drugs. J. Stud. Alcohol Drugs 74, 977–978 https://doi.org/10.15288/jsad.2013.74.977.
OECD, 2013. OECD guidelines for testing of chemicals.
Parolini, M., Ghilardi, A., Della Torre, C., Magni, S., Prosperi, L., Calvagno, M., Del Giacco, L., Binelli, A., 2017. Environmental concentrations of cocaine and its main metabolites modulated antioxidant response and caused cyto-genotoxic effects in zebrafish embryo cells. Environ. Pollut. 226, 504–514. https://doi.org/10.1016/j.envpol.2017.04.046.
Parveen, M., Azaz, S., Zafar, A., Ahmad, F., Silva, M.R., Silva, P.S.P., 2017. Structure elucidation, DNA binding specificity and antiproliferative proficiency of isolated compounds from Garcinia nervosa. J. Photochem. Photobiol. B Biol. 167, 176–188. https://doi.org/10.1016/j.jphotobiol.2016.12.035.
Passos, G.F.S., Gomes, M.G.M., de Aquino, T.M., de Araújo-Júnior, J.X., de Souza, S.J. M., Cavalcante, J.P.M., dos Santos, E.C., Bassi, Ê.J., da Silva-Júnior, E.F., 2020. Computer-Aided Design, Synthesis, and Antiviral Evaluation of Novel Acrylamides as Potential Inhibitors of E3–E2-E1 Glycoproteins Complex from Chikungunya Virus. Pharmaceuticals 13, 141. https://doi.org/10.3390/ph13070141.
Petzold, A.M., Balciunas, D., Sivasubbu, S., Clark, K.J., Bedell, V.M., Westcot, S.E., Myers, S.R., Moulder, G.L., Thomas, M.J., Ekker, S.C., 2009. Nicotine response genetics in the zebrafish. Proc. Natl. Acad. Sci. U. S. A. 106 (44), 18662–18667. https://doi.org/10.1073/pnas.0908247106.
Poklis, J.L., Devers, K.G., Arbefeville, E.F., Pearson, J.M., Houston, E., Poklis, A., 2014. Postmortem detection of 25I-NBOMe [2-(4-iodo-2,5-dimethoxyphenyl)-N-[(2-methoxyphenyl)methyl]ethanamine] in fluids and tissues determined by high performance liquid chromatography with tandem mass spectrometry from a traumatic death. Forensic Sci. Int. 234, e14–e20. https://doi.org/10.1016/j.forsciint.2013.10.015.
Polifka, J.E., Friedman, J.M., 1991. Teratogenic Effects of 'Recreational' Drugs Increasing the risk of congenital anomalies. Can Fam Physician 37, 1953–1962.
Prieto, D., Aparicio, G., Morande, P.E., Zolessi, F.R., 2014. A fast, low cost, and highly efficient fluorescent DNA labeling method using methyl green. Histochem. Cell Biol. 142 (3), 335–345. https://doi.org/10.1007/s00418-014-1215-0.
Ropero-Miller, J.D., Goldberger, B.A., 1998. Recreational drugs: Current trends in the 90s. Clin. Lab. Med. 18 (4), 727–746. https://doi.org/10.1016/S0272-2712(18)30148-3.
Roque Marques, K.M., do Desterro, M.R., de Arruda, S.M., de Araújo Neto, L.N., do Carmo Alves de Lima, M., de Almeida, S.M.V., da Silva, E.C.D., de Aquino, T.M., da Silva-Júnior, E.F., de Araújo-Júnior, J.X., de M. Silva, M., de A. Dantas, M.D., Santos, J.C.C., Figueiredo, I.M., Bazin, M.-A., Marchand, P., da Silva, T.G., Mendonça Junior, F.J.B., 2019. 5-Nitro-Thiophene-Thiosemicarbazone Derivatives Present Antitumor Activity Mediated by Apoptosis and DNA Intercalation. Curr. Top. Med. Chem. 19 (13), 1075–1091. https://doi.org/10.2174/1568026619666190621120304.
Ross, E.J., Graham, D.L., Money, K.M., Stanwood, G.D., 2015. Developmental consequences of fetal exposure to drugs: what we know and what we still must learn. Neuropsychopharmacology. 40 (1), 61–87. https://doi.org/10.1038/npp.2014.147.
Ross, P.D., Subramanian, S., 1981. Thermodynamics of protein association reactions: forces contributing to stability. Biochemistry 20 (11), 3096–3102. https://doi.org/10.1021/bi00514a017.
Santana, C.C., Silva-Júnior, E.F., Santos, J.C.N., Rodrigues, É.E.d.S., da Silva, I.M., Araújo-Júnior, J.X., do Nascimento, T.G., Oliveira Barbosa, L.A., Dornelas, C.B., Figueiredo, I.M., Santos, J.C.C., Grillo, L.A.M., 2019. Evaluation of guanylhydrazone derivatives as inhibitors of Candida rugosa digestive lipase: Biological, biophysical, theoretical studies and biotechnological application. Bioorg. Chem. 87, 169–180. https://doi.org/10.1016/j.bioorg.2019.03.030.
Sartorius, J., Schneider, H.J., 1997. Intercalation mechanisms with ds-DNA: Binding modes and energy contributions with benzene, naphthalene, quinoline and indole derivatives including some antimalarials. J. Chem. Soc. Perkin Trans. 2, 2319–2327. https://doi.org/10.1039/a702628e.
Savariz, F.C., Foglio, M.A., Goes Ruiz, A.L.T., da Costa, W.F., de Magalhães Silva, M., Santos, J.C.C., Figueiredo, I.M., Meyer, E., de Carvalho, J.E., Sarragiotto, M.H., 2014. Synthesis and antitumor activity of novel 1-substituted phenyl 3-(2-oxo-1,3,4-oxadiazol-5-yl) β-carbolines and their Mannich bases. Bioorg. Med. Chem. 22 (24), 6867–6875. https://doi.org/10.1016/j.bmc.2014.10.031.
Shanks, K.G., Sozio, T., Behonick, G.S., 2015. Fatal Intoxications with 25B-NBOMe and 25I-NBOMe in Indiana During 2014. J. Anal. Toxicol. 39 (8), 602–606. https://doi.org/10.1093/jat/bkv058.
Sourbron J., Schneider H., Kecskés A., Liu Y., Buening E.M., Lagae L., Smolders I., de Witte P. Serotonergic Modulation as Effective Treatment for Dravet Syndrome in a Zebrafish Mutant Model. ACS Chem Neurosci. 2016;7(5):588-98. doi: 10.1021/acschemneuro.5b00342
Stewart, A., Wong, K., Cachat, J., Gaikwad, S., Kyzar, E., Wu, N., Hart, P., Piet, V., Utterback, E., Elegante, M., Tien, D., Kalueff, A.V., 2011. Zebrafish models to study drug abuse-related phenotypes. Rev. Neurosci. 22, 95–105. https://doi.org/10.1515/RNS.2011.011.
Silva, M.M., Macedo, T.S., Teixeira, H.M.P., Moreira, D.R.M., Soares, M.B.P., da C. Pereira, A.L., de L. Serafim, V., Mendonça-Júnior, F.J.B., do Carmo A. de Lima, M., de Moura, R.O., da Silva-Júnior, E.F., de Araújo-Júnior, J.X., de A. Dantas, M.D., de O. O. Nascimento, E., Maciel, T.M.S., de Aquino, T.M., Figueiredo, I.M., Santos, J.C. C., 2018. Correlation between DNA/HSA-interactions and antimalarial activity of acridine derivatives: Proposing a possible mechanism of action. J. Photochem. Photobiol. B Biol. 189, 165–175. https://doi.org/10.1016/j.jphotobiol.2018.10.016.
Stewart, A.M., Cachat, J., Gaikwad, S., Robinson, K.S.L., Gebhardt, M., Kalueff, A.V., 2013. Perspectives on experimental models of serotonin syndrome in zebrafish. Neurochem. Int. 62 (6), 893–902. https://doi.org/10.1016/j.neuint.2013.02.018.
Subedi, B., Anderson, S., Croft, T.L., Rouchka, E.C., Zhang, M., Hammond-Weinberger, D.R., 2021. Gene alteration in zebrafish exposed to a mixture of substances of abuse. Environ. Pollut. 278, 116777. https://doi.org/10.1016/j.envpol.2021.116777.
Tang, M.H.Y., Ching, C.K., Tsui, M.S.H., Chu, F.K.C., Mak, T.W.L., 2014. Two cases of severe intoxication associated with analytically confirmed use of the novel psychoactive substances 25B-NBOMe and 25C-NBOMe. Clin. Toxicol. 52 (5), 561–565. https://doi.org/10.3109/15563650.2014.909932.
Tao, M., Zhang, G., Pan, J., Xiong, C., 2016. Deciphering the groove binding modes of tau-fluvalinate and flumethrin with calf thymus DNA.. Spectrochim. Acta - Part A Mol Biomol. Spectrosc. 155, 28–37. https://doi.org/10.1016/j.saa.2015.11.006.
Tao, M., Zhang, G., Xiong, C., Pan, J., 2015. Characterization of the interaction between resmethrin and calf thymus DNA in vitro. New J. Chem. 39 (5), 3665–3674. https://doi.org/10.1039/C4NJ02321H.
Vale, A., 2012. Drugs of abuse (amfetamines, BZP, cannabis, cocaine, GHB, LSD). Medicine (Baltimore). 40 (2), 84–87. https://doi.org/10.1016/j.mpmed.2011.11.018.
Verdonk, M.L., Cole, J.C., Hartshorn, M.J., Murray, C.W., Taylor, R.D., 2003. Improved protein-ligand docking using GOLD. Proteins Struct. Funct. Bioinforma. 52 (4), 609–623. https://doi.org/10.1002/prot.10465.
Viegas, A., Manso, J., Nobrega, F.L., Cabrita, E.J., 2011. Saturation-transfer difference (STD) NMR: A simple and fast method for ligand screening and characterization of protein binding. J. Chem. Educ. 88 (7), 990–994. https://doi.org/10.1021/ed101169t.
Wang, J., Yang, X., 2009. Multiplex binding modes of toluidine blue with calf thymus DNA and conformational transition of DNA revealed by spectroscopic studies. Spectrochim. Acta - Part A Mol Biomol. Spectrosc. 74 (2), 421–426. https://doi.org/10.1016/j.saa.2009.06.038.
Wood, D.M., Sedefov, R., Cunningham, A., Dargan, P.I., 2015. Prevalence of use and acute toxicity associated with the use of NBOMe drugs. Clin. Toxicol. 53 (2), 85–92. https://doi.org/10.3109/15563650.2015.1004179.
Xie, J., Chen, D., Wu, Q., Wang, J., Qiao, H., 2015. Spectroscopic analyses on interaction of melamine, cyanuric acid and uric acid with DNA. Spectrochim. Acta - Part A Mol Biomol. Spectrosc. 149, 714–721. https://doi.org/10.1016/j.saa.2015.04.060.

Xing L., Son J.H., Stevenson T.J., Lillesaar C., Bally-Cuif L, Dahl T., Bonkowsky J.L. A Serotonin Circuit Acts as an Environmental Sensor to Mediate Midline Axon Crossing through EphrinB2. J Neurosci. 2015;35(44):14794-808. doi: 10.1523/JNEUROSCI.1295-15.2015

Yang, H., Tang, P., Tang, B., Huang, Y., Xiong, X., Li, H., 2017. Novel poly(ADP-ribose) polymerase inhibitor veliparib: biophysical studies on its binding to calf thymus DNA. RSC Adv. 7 (17), 10242–10251. https://doi.org/10.1039/C6RA28213J.

Zhang, C., Wang, J., Zhang, S., Zhu, L., Du, Z., Wang, J., 2017. Acute and subchronic toxicity of pyraclostrobin in zebrafish (Danio rerio). Chemosphere 188, 510–516. https://doi.org/10.1016/j.chemosphere.2017.09.025.

Zhang, C., Zhang, J., Zhu, L., Du, Z., Wang, J., Wang, J., Li, B., Yang, Y., 2020. Fluoxastrobin-induced effects on acute toxicity, development toxicity, oxidative stress, and DNA damage in Danio rerio embryos. Sci. Total Environ. 715, 137069. https://doi.org/10.1016/j.scitotenv.2020.137069.